ELSEVIER

International Journal of Fatigue 23 (2001) 499–507

International Journal of Fatigue

www.elsevier.com/locate/ijfatigue

The fatigue strength of sandwich beams with an aluminium alloy foam core

A.-M. Harte, N.A. Fleck *, M.F. Ashby

Cambridge Centre for Micromechanics, Cambridge University Engineering Department, Trumpington Street, Cambridge CB2 1PZ, UK

Received 17 July 2000; received in revised form 25 January 2001; accepted 25 January 2001

Abstract

Sandwich beams with aluminium face sheets and an aluminium alloy foam core are tested in cyclic four point bend, and S–N fatigue curves are determined for the failure modes of face fatigue, core shear and core indentation. The operative failure mode is dictated by the relative fatigue strength of face sheets to core, and upon the geometry of the sandwich beams. Simple analytical models are developed to predict the fatigue strength for each of the competing failure modes, and a design map is produced to display the fatigue strength and mode of failure as a function of sandwich beam geometry.

Keywords: Sandwich beam fatigue; Limit load analysis; Metal foams; Fatigue design

1. Introduction

Sandwich beams and panels are common lightweight structures: by separating two stiff and strong skins by a light core, an efficient structure is obtained. Typical applications include boat hulls, jet-engine nacelles, satellite panels and the cladding of buildings. In almost all applications, loading is cyclic in nature and so the fatigue strength of the sandwich beam or panel is of concern. To date, the cores used in sandwich construction have been largely limited to balsa wood, polymeric foams, and aluminium or polyamide honeycombs; however, recent advances in manufacturing techniques for foamed metals have led to a sufficiently consistent product for structural applications. Currently, the most widely used foamed alloys are aluminium casting alloys due to their relatively low melting temperature, good foamability and low density. Aluminium foams have potential to replace polymer foams in sandwich panel applications due to their increased specific stiffness and higher temperature capability.

In this paper, sandwich beams, made from Alporas[1] aluminium alloy foam core and half-hard commercially pure aluminium face sheets, are loaded in repeated four point bend in order to explore the failure mechanisms in fatigue. Alporas foam is a closed cell aluminium alloy, of relative density (density of the foam divided by the density of the cell wall material) $\hat{\rho}$=11%, and average cell size 3 mm. The cell walls contain about 5% calcium in order to increase its viscosity in the molten state: the phase diagram for aluminium–calcium indicates a eutectic near this composition [1].

Three modes of failure have been observed in monotonic four point bend loading, depending upon the geometry of the sandwich beams: face-sheet yield, core shear and core indentation [2–4]. A negligible literature exists however on the fatigue of sandwich panels with a metal foam core. The fatigue behaviour of sandwich beams comprising composite face-sheets and a polymer foam core has been reported by Burman and Zenkert [5,6], and Olsson and Lönnö [7]; in these studies, fatigue failure was by core shear. Here, the main competing modes of fatigue failure are explored.

The structure of this paper is as follows. First, the

* Corresponding author. Tel.: +44-1223-332-650; fax: +44-1223-332-662.

E-mail address: naf1@eng.cam.ac.uk (N.A. Fleck).

[1] European supplier: Karl Bula, Innovation Services, Ch-5200 Brugg, Herrenmatt 7F, Switzerland.

0142-1123/01/$ - see front matter
PII: S0142-1123(01)00012-3

shear fatigue properties of Alporas aluminium alloy foam are measured, and compared with existing data from the literature on tension–tension and compression–compression fatigue. Second, limit load analytical methods are used to predict the fatigue strength of sandwich beams comprising metallic face-sheets and metallic foam cores under four point bend loading by circular rollers. Predictions are given for failure by face-sheet fatigue, core shear fatigue and progressive indentation beneath the rollers, and the competing failure modes are summarised in a design map. Third, sandwich beams comprising an Alporas foam core and half-hard aluminium face-sheets are subjected to cyclic loading, and the failure modes are determined for a number of beam geometries. Finally, the predicted fatigue strengths are compared with the measured values in order to provide support for the limit load analyses.

2. Review of the monotonic and cyclic strength of Alporas foam

Before developing limit load expressions for the fatigue strength of sandwich beams we first review the monotonic and cyclic behaviours of Alporas foam, based on the studies of Harte et al. [8] and Sugimura et al. [9]. The monotonic tensile, compressive and shear nominal stress versus nominal strain curves are summarised in Fig. 1, taken from Harte et al. [8] and Chen et al. [3].

In monotonic tension, a strong strain hardening behaviour is exhibited, prior to tearing across the section at a nominal strain of only a few percent. The foam is almost isotropic, with a Young's modulus E=1.0 GPa, Poisson's ratio ν=0.3, and a nominal tensile strength σ_{pl}=1.85 MPa. Consistent with the strong strain hardening response prior to the onset of tearing, the strain state was observed to be relatively uniform, with no evidence of localisation of deformation into a band prior to tearing.

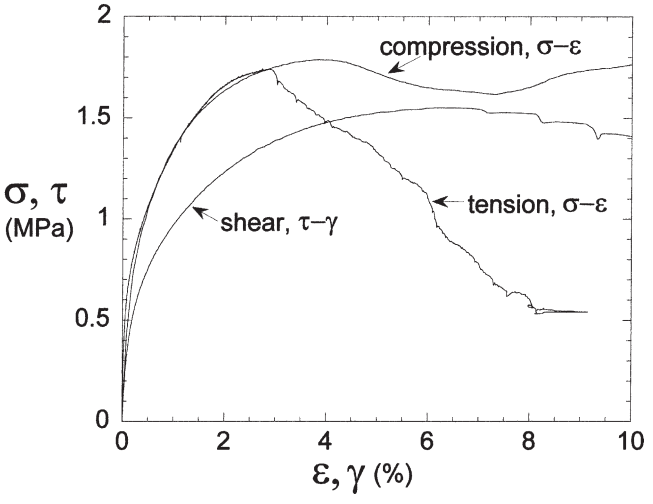

Fig. 1. Nominal stress versus nominal strain uniaxial response of Alporas foam, of relative density $\hat{\rho}$=11%.

The monotonic shear response of Alporas has been explored by Chen et al. [3] using a double lap shear geometry. The response is qualitatively similar to that displayed in tension, see Fig. 1, with spatially uniform straining until fracture. Fracture is by the initiation, growth and coalescence of tensile microcracks along the mid-plane of the specimen, with each microcrack inclined at about 45° to the shearing direction. The peak shear strength τ_{pl}=1.56 MPa is attained at a shear strain of about 8%.

In monotonic compression, Alporas progressively shortens by the formation of a sequence of transverse crush bands, each of thickness about one cell dimension. Crushing initiates on the weakest plane, followed by the next weakest plane, and so on until the whole specimen has attained a compressive nominal strain of about 30%. During this phase of random crush band formation the nominal stress–strain curve oscillates about an average plateau value of σ_{pl}=1.85 MPa, with the nominal compressive strain increasing from 2 to 30% (not shown). Subsequent shortening occurs in an almost uniform manner: the opposing faces of individual cell walls touch, and the material progressively locks-up with a steepening stress–strain response. It is noted from Fig. 1 that the plateau strength is significantly higher than the initial yield strength (of about 0.3 MPa), as defined by the point where the stress–strain curve first becomes non-linear.

In tension–tension fatigue the specimens lengthen progressively with increasing fatigue cycles, until they fail at an axial extension of 1–2%, equal to the monotonic ductility. A typical stress versus life, S–N curve, for Alporas foam of relative density $\hat{\rho}$=11% is shown in Fig. 2(a), for a load ratio R=0.1 in tension and R=10 in compression, where R is defined by the ratio of the minimum stress σ_{min} and maximum stress σ_{max} of the fatigue cycle,

$$R=\frac{\sigma_{min}}{\sigma_{max}} \quad (1)$$

The observed S–N response is typical of that for structural materials: the fatigue life decreases with increasing stress level, and the data may be fitted by a straight-line on a log-linear plot. The fatigue strength attains a plateau value, termed the *endurance strength*, at about 10^7 cycles [8–10].

The cyclic compression–compression response depends somewhat upon the degree of heterogeneity of the foam. Harte et al. [8] tested an Alporas foam of relatively homogeneous microstructure, and found that a single crush band forms after an incubation number of cycles N_f and then broadens with additional fatigue cycles. In contrast, Sugimura et al. [9] tested an Alporas foam of more heterogeneous microstructure, and found that a sequence of randomly located crush bands developed after the initial band. In both studies, the incu-

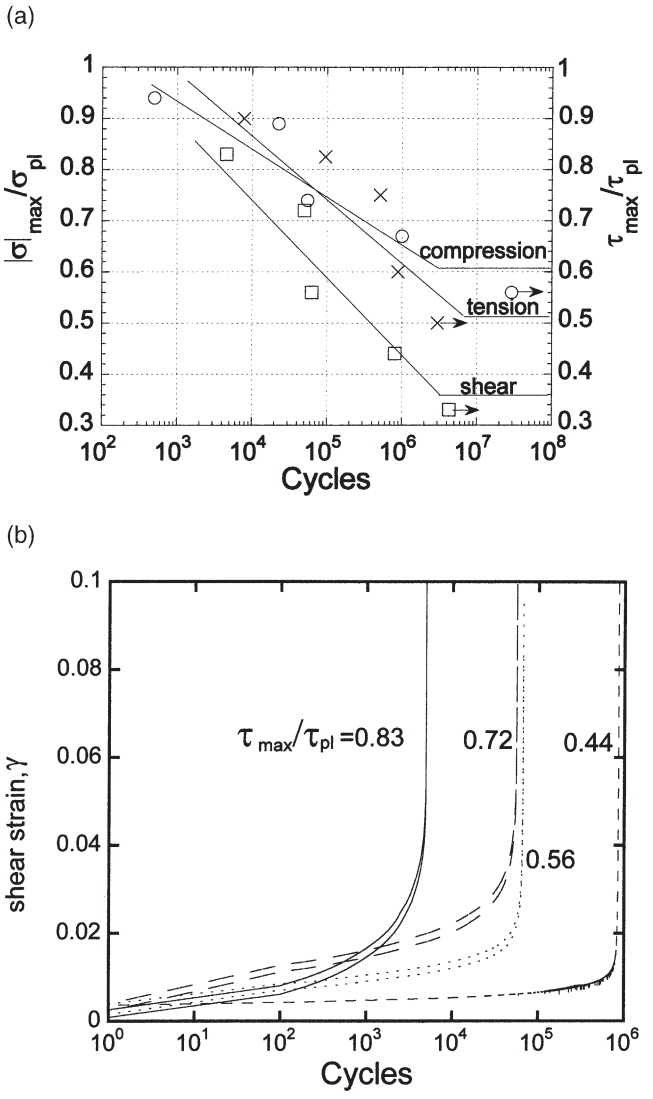

Fig. 2. (a) S–N curves for Alporas foam $\hat{\rho}$=11% in tension (R=0.1), compression (R=10) and shear (R=0.1). (b) Accumulated shear strain with cycles for Alporas foam $\hat{\rho}$=11% in fatigue with R=0.1.

bation number of cycles N_f was defined as the number of fatigue cycles up to the point where the rate of specimen shortening accelerated and the first crush band was nucleated. The nominal compressive strain at the end of the incubation period was equal to about 2%. On taking the incubation period N_f as the fatigue life, a S–N curve can be constructed; a typical example is shown in Fig. 2(a) for a load ratio R=10, taken from Harte et al. [8].

2.1. Shear fatigue of Alporas

The shear response of metallic foams is of particular concern as the core of a sandwich beam is loaded predominantly in shear. Shear fatigue tests have been performed on Alporas, at a load ratio R=0.1, using the same specimen geometry as that of Chen et al. [3] for monotonic shear: fatigue tests were performed at 20 Hz on specimens of dimension 100×20×20 mm. The fatigue response is summarised in curves of accumulated shear strain versus number of cycles N at selected levels of shear stress τ_{max} see Fig. 2(b). In labelling the data, the maximum nominal shear stress τ_{max} in each test has been normalised by the peak stress τ_{pl} of the monotonic shear stress–strain curve of Fig. 1. As for the monotonic tests, the fatigue response is qualitatively similar to the tensile case: during an initial incubation period N_f the shear strain increases to about 2% with increasing number of loading cycles. A sharp increase in the rate of strain accumulation then occurs with failure shortly thereafter. As for the tensile specimens, no sign of damage appears within the specimen during the incubation period. The first visible cracks appear in the faces of the cells at the end of the incubation period. These tensile microcracks are inclined at about 45° to the overall direction of shear, as for the case of monotonic shear. The cell edges then fail and the individual microcracks link up on a single overall failure surface along the mid-plane of the specimen.

A plot of normalised shear stress τ_{max}/τ_{pl} versus fatigue life N_f has been added to the S–N plot of Fig. 2(a). As for the tensile and compressive fatigue cases, the fatigue life increases with reducing stress level, and a fatigue limit is exhibited at about 10^7 cycles [8–10]. It is noted from Fig. 2(a) that the normalised *endurance strength* at the fatigue limit is τ_{max}/τ_{pl}=0.35, which is much lower than the values observed in tensile and in compressive fatigue: for compression–compression fatigue, we note that $|\sigma|_{max}/\sigma_{pl}$=0.6 where σ_{pl} is the compressive plateau strength of the foam. And for tension–tension fatigue, σ_{max}/σ_{pl} equals 0.5, where σ_{pl} is the peak tensile strength.

3. Sandwich beam design

Analytical upper bound formulae for the collapse strength of sandwich beams in four point bending have been derived by Ashby et al. [10] upon treating both core and face sheets as rigid-ideally plastic beams. We shall estimate the fatigue strength of the sandwich beams at infinite life (i.e. N_f=10^7 cycles) by replacing the monotonic strength of the foam core and face sheets in these strength formulae by their respective *endurance strengths*; here, we continue with the operational definition of endurance strength as the cyclic strength at a fatigue life of 10^7 cycles. The rationale for this modification to the strength formulae for sandwich beams is as follows. It is clear from the previous section that the fatigue failure of Alporas foam is by a material ratchetting mechanism, such that the mean strain of the fatigue cycle increases progressively with the number of fatigue cycles. The fatigue life of the foam N_f, at any prescribed level of cyclic stress, is defined by the knee in the curve

of accumulated strain versus cycles; at this point, the strain increases dramatically in a manner analogous to plastic collapse. Thus, formulae for the sandwich beam fatigue strength at a fatigue life of 10^7 cycles can be obtained from the equivalent limit load formulae provided the monotonic plateau strength of the foam is replaced by its endurance strength.

3.1. Fatigue failure modes of sandwich beams

The underlying concept in sandwich beam design is to separate the thin, strong face sheets by a lightweight core. The beam carries bending moments mainly by membrane action of the face sheets, while the transverse shear force in the beam is equilibrated by shear stresses within the core. Consider the monotonic loading of a sandwich beam in 4-point bend by circular rollers, as sketched in Fig. 3. The beam may fail by face yield, by core shear or by additional collapse mechanisms such as local indentation beneath the loading rollers.

We shall modify the limit load analysis to predict the fatigue strength at infinite life (that is, at least 10^7 cycles) for the three failure modes of face fatigue, core shear fatigue and core indentation fatigue. The face sheets are idealised as rigid, ideally plastic solids of tension–tension endurance strength $\sigma_{max}=\sigma_e^f$, where the subscript e refers to endurance strength (at 10^7 cycles) and the superscript f refers to face sheet. Similarly, the foam core is treated as a rigid, ideally plastic solid of compression–compression fatigue strength $|\sigma|_{max}=\sigma_e^c$, and shear fatigue strength $|\tau|_{max}=\tau_e^c$, where the superscript c refers to the core.

3.1.1. Face fatigue

When the face sheets comprise a material of low fatigue strength then it is expected that the maximum load of the fatigue cycle F_f at the endurance limit of the sandwich beam is set by face fatigue. The simplest approach is to assume that cyclic collapse occurs when the stress in the face sheets attains the maximum stress of the fatigue cycle at 10^7 cycles, here termed the endurance strength σ_e^f. For four point bend loading the collapse load is determined by equating the maximum bending moment within the sandwich beam to the collapse moment of the section, giving

$$F_f=\frac{4bt(c+t)}{\ell-S}\sigma_e^f \tag{2}$$

where the small fraction of load carried by the core has been neglected.

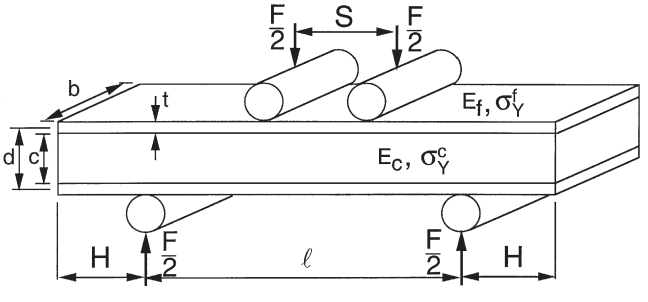

Fig. 3. Schematic of the geometry of the sandwich beam and the loading rollers.

3.1.2. Indentation fatigue

Ashby et al. [10] argue that the indentation mode of monotonic collapse involves the formation of three plastic hinges within the top face sheet adjacent to each indenter, with compressive yield of the underlying core, as sketched in Fig. 4. The equivalent mode in fatigue is associated with fatigue failure in bending of the face sheet and simultaneous fatigue failure of the underlying core in compression.

The maximum load of the fatigue cycle, $F_I/2$ on each roller, can be derived by a simple upper bound calculation, wherein two segments of the upper face of wavelength λ are rotated through a small angle θ. The resulting collapse load is given by

$$\frac{F_I}{2}=\frac{4M_p}{\lambda}+\lambda b\sigma_e^c \tag{3}$$

where $M_p=\sigma_e^f bt^2/4$ is the collapse moment for fatigue failure of the face-sheet, and the strength of the core is equated to its endurance strength σ_e^f. Minimisation of this upper bound solution for F_I with respect to the free parameter λ gives the fatigue indentation load F_I of

$$F_I=4bt\sqrt{\sigma_e^c\sigma_e^f} \tag{4}$$

at the wavelength

$$\lambda=t\sqrt{\frac{\sigma_e^f}{\sigma_e^c}} \tag{5}$$

3.1.3. Core shear

When a sandwich beam is subjected to a monotonic transverse shear force plastic collapse can occur by core shear. Two competing collapse mechanisms can be identified, as shown in Fig. 5 for a beam in four point bending. Mode A comprises plastic hinge formation under the inner rollers with shear yielding of the core. Mode B consists of plastic hinge formation both at the

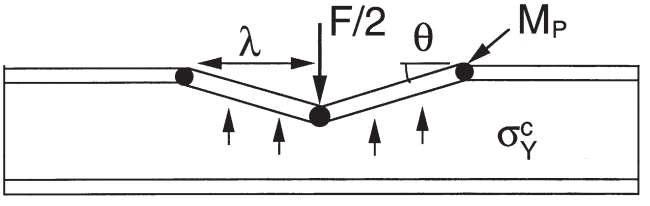

Fig. 4. Schematic of a sandwich beam undergoing core indentation.

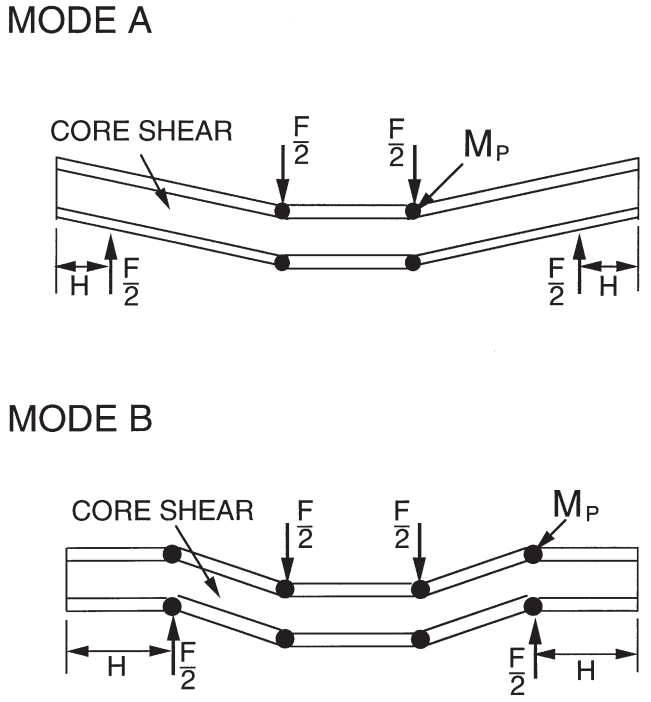

Fig. 5. Schematic of a sandwich beam undergoing Mode A and Mode B core shear.

inner and outer supports. Whether Mode A or Mode B dominates depends on the length of the sandwich beam overhang H beyond the outer rollers. If the load to form a set of hinges at the outer rollers is lower then the load required to shear the core between the outer rollers and the specimen ends then Mode B will dominate.

Similar collapse modes can occur under cyclic loading. Cyclic core shear is by fatigue failure of the core with simultaneous fatigue failure of the face sheets in bending at the hinge locations. A simple upper bound calculation can be performed to calculate the maximum load of the fatigue cycle for Modes A and B by equating the external work done to the energy dissipated within the plastic hinges of the face sheets and by shearing of the core. For Mode A, the peak load F_A is

$$F_A=2\frac{bt^2}{\ell-S}\sigma_e^f+2bc\left(1+\frac{2H}{\ell-S}\right)\tau_e^c \tag{6}$$

Similarly, for Mode B, the peak load is

$$F_B=4\frac{bt^2}{\ell-S}\sigma_e^f+2bc\tau_e^c \tag{7}$$

from which the transition overhang to trigger mode B is $H_t=\sigma_e^f t^2/2c\tau_e^c$. The corresponding transition overhang for monotonic loading is given by $H_t=\sigma_y^f t^2/2c\tau_{pl}^c$, where σ_y^f is the yield strength of the face sheets and τ_{pl}^c is the peak shear strength of the core. In general, the ratio σ_y^f/τ_{pl}^c is different from the ratio σ_e^f/τ_e^c for a given material combination and so the transition overhang for fatigue loading is different from that for monotonic loading.

3.2. Design maps for sandwich beams

It is assumed that the operative collapse mechanism for a sandwich beam is the one associated with the lowest fatigue limit. This is shown graphically in Fig. 6 by plotting contours of normalised cyclic failure load $\bar{F}=F/\sigma_e^f b(\ell-S)$ on a diagram with axes $c/(\ell-S)$ and t/c, for values of σ_e^f, σ_e^c and τ_e^c representative of those for Alporas foam core and half-hard aluminium face sheets. Regimes of dominance of cyclic collapse mechanism are included on the map. We deduce from Fig. 6 that core shear fatigue dominates the map. Face fatigue occurs when $t\ll(\ell-S)$, and cyclic indentation occurs when $t\ll c$ and $c>0.1(\ell-S)$. The map also includes the failure regimes for monotonic loading. It is seen that the core shear regime is somewhat larger for cyclic loading than for monotonic loading; this is a consequence of the fact that the ratio of endurance strength to monotonic strength is least for the case of shear loading of the foam core.

4. Experimental investigation of sandwich beam fatigue

The fatigue failure map for a sandwich beam in 4-point bending as given in Fig. 6 was used to design a

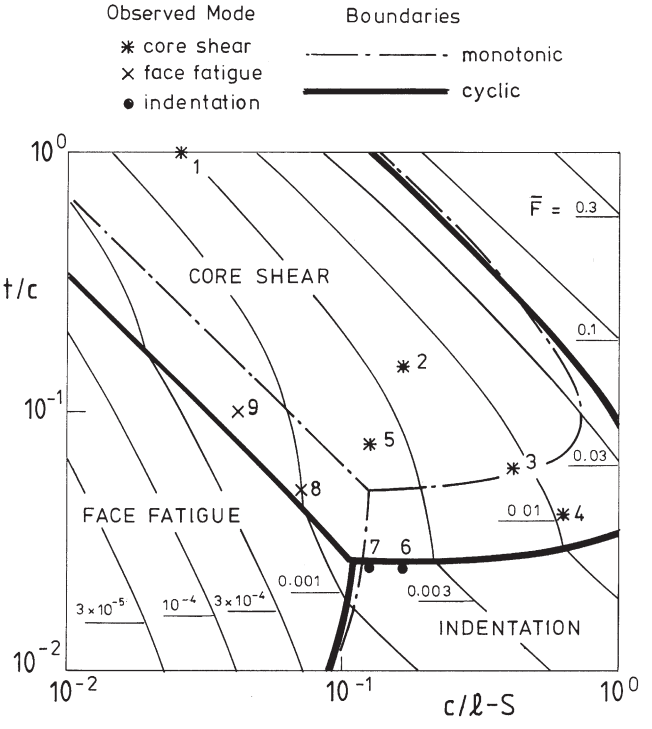

Fig. 6. Failure mode maps with contours of normalised cyclic failure load $\bar{F}=F/\sigma_e^f b(\ell-S)$ for sandwich beams in cyclic four point bend with $\sigma_Y^c/\sigma_Y^f=0.02$. (*) Core shear, (×) face fatigue, (●) indentation. The bold line is the boundary for cyclic loading and the thin chain-dotted line is the boundary for monotonic loading.

set of fatigue experiments: the accuracy of the limit load analysis was thereby assessed. The 4-point bend geometry has the advantage that it subjects a beam to a constant bending moment and zero shear force between the centre rollers. This decouples the failure mechanisms and simplifies experimental observation: face fatigue occurs between the central rollers, core shear takes place between inner and outer rollers, and indentation occurs directly beneath the rollers.

4.1. Materials

Sandwich beams of width b=50 mm were manufactured by bonding aluminium face-sheets to Alporas foam of relative density $\hat{\rho}$=11%, and were then tested in four-point bend using circular rollers of diameter 19 mm. The face-sheets were half-hard, commercial-purity aluminium sheets of thickness t=0.5, 1.0, 1.5 and 3.0 mm. The aluminium face-sheets were degreased and abraded, and were then adhered to the foam core using Hexcel Redux 322 epoxy adhesive on a nylon carrier mesh. The sandwich beams were air cured at 175°C for 1 h, and bonding was facilitated by imposing dead-loading with a nominal contact pressure of 0.01 MPa. The shear strength of the cured Redux 322 adhesive was taken to be 20 MPa, from Hexcel's data sheets[2]. (This strength is about one order of magnitude higher than that of the Alporas foam, and so no adhesive failure was observed.)

The mechanical properties of the face sheets and core were measured as follows. Tensile specimens of dog-bone geometry were cut from the aluminium face sheets, with the longitudinal direction parallel to the rolling direction of the sheet, and appropriately strain-gauged. All face sheets of a given thickness were taken from the same rolled sheet. The tensile nominal stress–strain curves for all four thicknesses are summarised in Fig. 7. Repeat tests confirmed that the scatter in stress–strain response was negligible for face sheets of any given thickness. However, the yield strength varies by up to 20% with thickness of sheet, and the tensile ductility lies in the range 0.7–2%. Checks revealed that the tensile stress–strain curves of the face sheets were not affected by the thermal cycle associated with bonding of the face sheets to the foam core. The Young's modulus was confirmed to be E_f=69 GPa for all thicknesses, and the assumed Poisson ratio was ν_f=0.3. The endurance strength of the aluminium face sheet material in tension–tension fatigue was measured to be σ_{max}=63 MPa at a load ratio R=0.1 for dog-bone specimens of thickness 3.0 mm. The endurance strength for other thicknesses was then deduced by scaling in proportion to the respective yield strengths.

[2] Hexcel publication RTC020 on Redux 322 adhesive, January 1997, Hexcel, Duxford, Cambridge, CB2 4QD, UK.

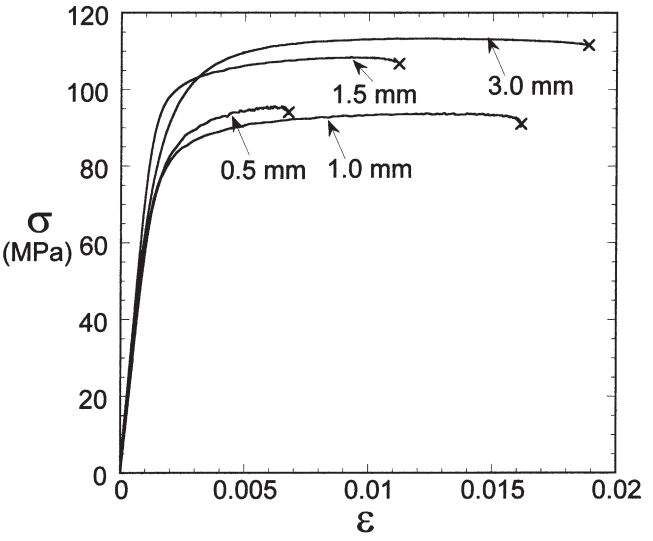

Fig. 7. Nominal stress–nominal strain for the commercially pure half-hard aluminium skins. Tension tests were done on dog-bone specimens made out of 0.5, 1.0, 1.5 and 3.0 mm sheet in the roll direction.

4.2. Test method

The sandwich geometries tested are summarised in Table 1. The dependence of the fatigue failure mode upon geometry was investigated by changing the thickness of the skin, t, the thickness of the core, c, and the distance between the inner and outer rollers, $\ell - S$. A detailed study was made for three geometries chosen to lie well within the domains of face fatigue (geometry number 8), core shear (geometry number 2) and indentation (geometry number 6).

The fatigue tests were performed at 20 Hz using a ratio of minimum applied load to maximum applied load, $R=F_{min}/F_{max}$=10. Additional fully reversed tests (R=−1) were performed using a tension–compression bend rig of design similar to that used by Burman and Zenkert [5]. In order to avoid excessive specimen rattle on load reversal in the fully reversed tests, it was necessary to clamp the sandwich beam between two steel plates of width 20 mm instead of using roller-support. Consequently, for the fully reversed case, the possible failure modes were limited to core shear or to face sheet fatigue.

5. Experimental results

5.1. Fatigue tests of sandwich beams

Plots of accumulated displacement versus number of fatigue cycles for specimens failing by indentation, face fatigue and core shear are shown in Fig. 8(a–c); results are presented for R=10 at selected values of peak load F_{max}, after normalisation by the peak load F_{pl} from a monotonic test on the same geometry. Typically, the

Table 1
Sandwich panels tested in fatigue loading

Specimen[a]	c (mm)	t (mm)	ℓ (mm)	S (mm)	Failure mode[b]	$10^3\ \bar{F}$ (measured)	$10^3\ \bar{F}$ (calculated)
1	3.0	3.0	220	100	CS (A)	2.16	2.68
2	20.0	3.0	220	100	CS (B)	5.77	5.34
3	50.0	3.0	220	100	CS (B)	10.5	9.58
4	75.0	3.0	220	100	CS (B)	13.5	13.1
5	20.0	3.0	220	60.0	CS (B)	3.97	2.47
6	20.0	1.5	220	100	IND	4.33	2.18
7	20.0	0.5	290	130	IND	2.52	1.63
8	10.0	0.5	260	60.0	FF	0.883	0.572
9	10.0	1.0	430	190	FF	0.991	0.799

[a] Each specimen has a length of 300 mm except for No. 9 which is 500 mm long.
[b] CS(A/B): core shear, mode A or B; IND: indentation; FF: face fatigue. All observed failure modes are consistent with those predicted.

fatigue response comprised a slow rate of accumulation of roller deflection with increasing cycles, until at the end of the incubation period, the rate of roller deflection increased dramatically. The fatigue life was defined as the incubation period N_f at any given load level.

Photographs of the specimens failing by face fatigue, indentation and core shear are given in Fig. 9(a–c) and the corresponding points are indicated as geometries 8, 6 and 2, respectively, on the failure mode map, Fig. 6. The fatigue life in each of these tests was about 4×10^6 cycles. The details of damage development are as follows.

1. Indentation fatigue was progressive in nature, with the rate controlled by the compaction of the foam core immediately beneath the rollers. A crush band initiated at the knee of the deflection-cycles curves of Fig. 9(a), and broadened with additional loading cycles. This behaviour is similar to that noted by Harte et al. [8] for the uniaxial compression of Alporas foam.
2. Face fatigue occurred by the tensile separation of the tensile face sheet. A sharp knee in the deflection-cycles curve was due to the rapid propagation of a fatigue cracks across the face sheet on the tensile side of the beam.
3. For the case of failure by core shear, Fig. 9(c), the cell faces underwent microcracking at the beginning of the knee of the deflection-cycles curve. These microcracks were of a tensile nature and were inclined at an angle of approximately 45° to the neutral axis. Eventually a set of the microcracks coalesced along the mid-plane of the core. In some cases the plane of microcrack coalescence was located off-centre; it is thought that this was due to some variability of strength within the foam core.

The qualitative fatigue response at $R=-1$ is similar to that shown at $R=10$ for the specimens failing by core shear, and loaded by circular rollers. Microcracking occurred between the inner and outer supports (in the zone of constant shear force) and was concentrated along the neutral axis of the core. The tensile microcracks were inclined at ±45° to the neutral axis, and coalesced along the neutral plane.

5.2. S–N curves

The S–N curves for a selection of the sandwich beams are shown in Fig. 10, with regression lines added to show the overall trends. The fatigue limit for face fatigue (specimen 8) is the highest, followed by indentation (specimen 6) and core shear (specimen 2). This is consistent with the fact that face fatigue is governed by the tensile behaviour of the skins, indentation by the compressive response of the core and core shear by the shear response of the core. The S–N curve for $R=-1$ has a fatigue limit which is significantly lower than the core shear case at $R=10$. The above results suggest that fatigue is a major consideration in the design of sandwich beams (and panels) with a metallic foam core. Extrapolation of the log–log S–N data for both the sandwich beam tests (Fig. 10) and the foam fatigue tests [Fig. 2(a)] generally gives a strength at one loading cycle in excess of the monotonic strength; thus, it is expected that the full S–N curves measured down to low numbers of loading cycles would exhibit an inverse S-shape rather than a bilinear shape. In the current study, it was assumed that the high cycle fatigue regime was of more immediate practical relevance, and so fatigue tests were performed only for lives in excess of about 1000 cycles.

6. Comparison of predictions with experimental results

Fatigue tests were performed on all geometries listed in Table 1, and the fatigue limit was determined for each

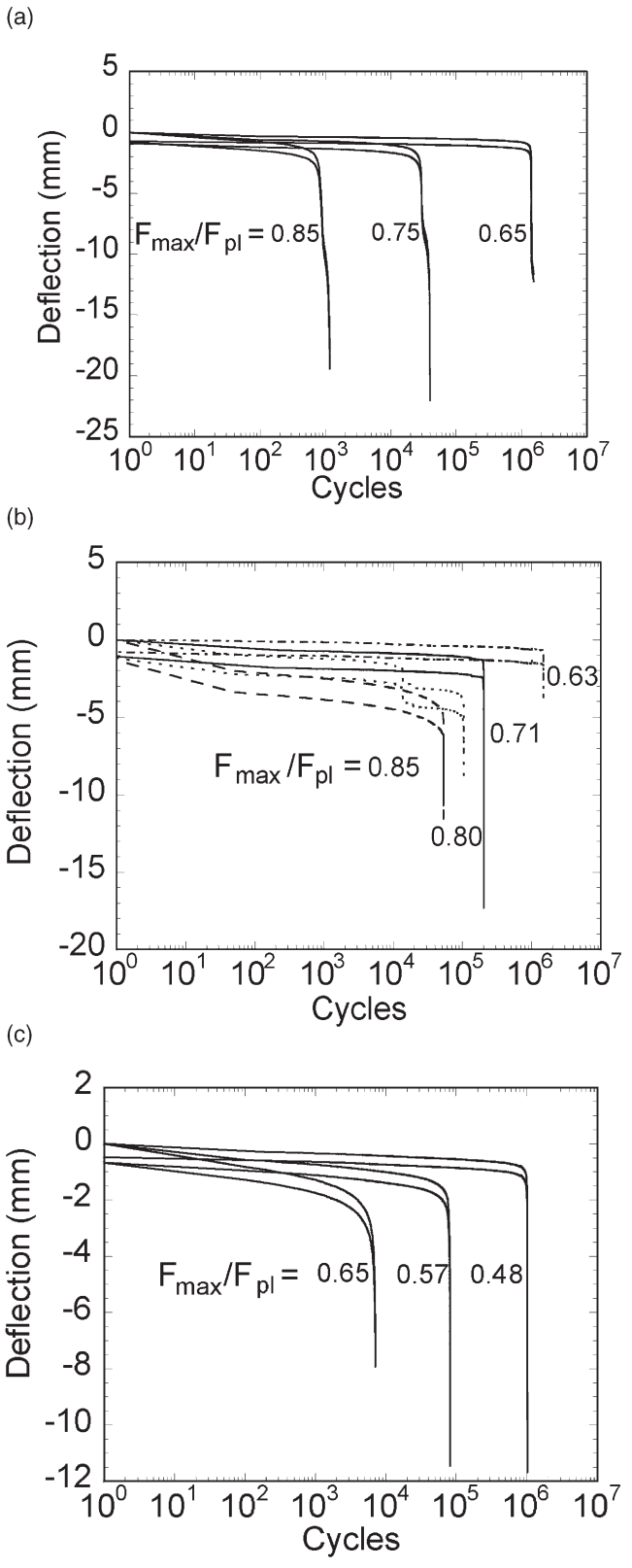

Fig. 8. Deflection versus number of cycles for a sandwich beam in four point bend fatigue that fails by (a) indentation, (b) face fatigue and (c) core shear, R=10.

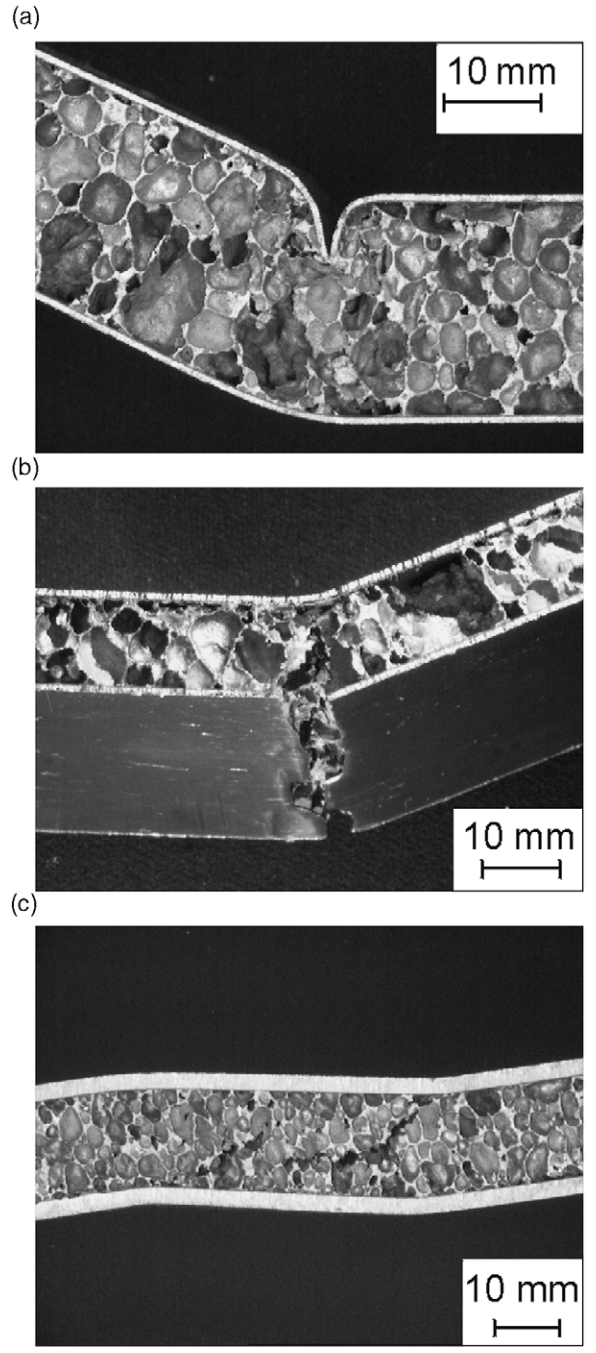

Fig. 9. The observed failure modes in fatigue: (a) indentation, (b) face fatigue and (c) core shear. In the case of core shear, inclined microcracks coalesce along the mid-plane of the foam core, in the regions of the beam between the inner and outer supports which carry transverse shear loads.

geometry by increasing the fatigue load in increments of 10% until failure occurred at about 10^7 cycles. The observed fatigue failure mode is included on the failure mode map in Fig. 6 and in Table 1, and the measured and predicted fatigue strengths are compared in Table 1.

It is seen from Fig. 6 and Table 1 that the theoretical predictions of the operative fatigue mode and associated

fatigue strength are, in general, in reasonable agreement with the observations. For example, geometries 1–5 all failed by core shear in fatigue. A comparison of the predicted fatigue strengths for mode A via (6) and for mode B via (7) suggest that geometry 1 fails by mode A, whereas geometries 2–5 fail by mode B; the observed failure modes support these predictions. Under monotonic loading, geometries 1 to 3 and 5 underwent core shear while geometry 4 suffered indentation; such behaviour is predicted by the failure map. Specimen 7 failed by the combined mode of face yield and indentation under monotonic loading, in agreement with the prediction that this geometry is on the boundary between both collapse modes. Under cyclic loading, this geometry lies within the indentation regime, and failure was by cyclic indentation alone.

There are some discrepancies, however, between the predicted and observed failure modes. Specifically, geometries 8 and 9 lie close to the theoretical boundary between face fatigue and core shear, and failed by face fatigue rather than by the predicted mode of core shear. The measured fatigue strengths for indentation (geometries 6 and 7) were nearly twice the predicted values for indentation. A similar discrepancy has been noted previously by Chen et al. [3] for monotonic indentation and is due to the increased indentation strength of a metallic foam when bonded to face-sheets. The cell edges are supported against plastic hinge formation by the encastre-support of the adhesive.

7. Concluding remarks

This combined experimental and theoretical study has shown that a reduction in the strength of sandwich beams exists for cyclic loading compared to monotonic loading. The set of possible collapse mechanisms do not change however: failure is by face sheet yield/fatigue, by core sehar or by indentation beneath the rollers. The existing analytical formulae of Ashby et al. [10] can be modified for the fatigue case by making use of S–N fatigue data for the face sheets and the metal foam core. Cyclic loading reduces the shear strength of Alporas foam by a factor of about 3 at R=0.1 and by a factor of about 6 at R=−1; this implies that sandwich beams are particularly prone to core shear under cyclic loading.

Acknowledgements

The authors are grateful to DARPA/ONR for their financial support through MURI grant number N00014-1-96-1028 on the Ultralight Metal Structures project at Harvard University. A-M. H. also wishes to thank the Newton Trust for financial support.

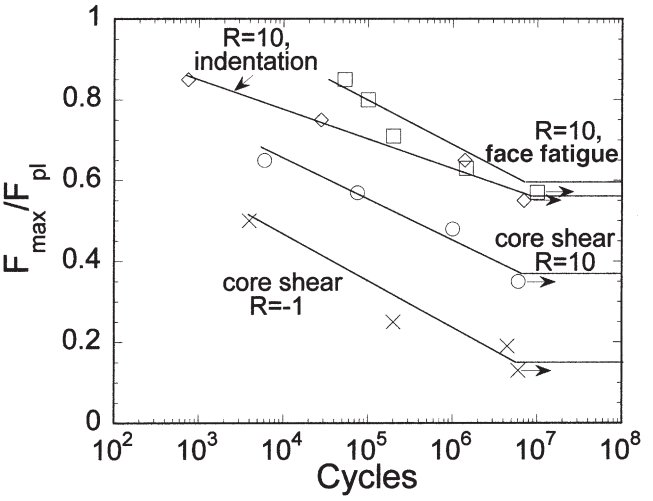

Fig. 10. S–N curves for the sandwich beams in four point bend, failing face fatigue, indentation and core shear.

References

[1] Miyoshi T, Itoh M, Akiyama S, Kitahara A. Aluminium foam, 'Alporas': the production process, properties and applications. In: Banhart J, Ashby MF, Fleck NA, editors. Proceedings of Metal Foams and Porous Metal Structures. Bremen, Germany: Verlag MIT Publications, 2000:125–32.

[2] Bart-Smith H, Hutchinson JW, Evans AG. Measurement and analysis of the structural performance of cellular metal sandwich construction. International Journal of Mechanical Sciences 2001, submitted for publication.

[3] Chen C, Harte A-M, Fleck NA. The plastic collapse of sandwich beams with a metallic foam core. International Journal of Mechanical Sciences, 2001, submitted for publication.

[4] McCormack TM, Miller R, Kesler O, Gibson LJ. Failure of sandwich beams with metallic foam cores. International Journal of Mechanical Sciences, 2001, submitted for publication.

[5] Burman M, Zenkert D. Fatigue of foam core sandwich beams—1: undamaged specimens. Int J Fat 1997;19(7):551–61.

[6] Burman M, Zenkert D. Fatigue of foam core sandwich beams—1: effect of initial damage. Int J Fat 1997;19(7):563–78.

[7] Olsson K-A, Lonno A. Test procedures for foam core materials. In: Olsson K-A, Reichard RP, editors. First International Conference on Sandwich Construction. Solihull, UK: EMAS Ltd, 1989:293–318.

[8] Harte A-M, Fleck NA, Ashby MF. Fatigue failure of an open and a closed cell aluminium alloy foam. Acta Mater 1999;47(8):2511–24.

[9] Sugimura Y, Rabiei A, Evans AG, Harte AM, Fleck NA. Compression fatigue of cellular Al alloys. J Mat Sci Eng A 1999;A269:38–48.

[10] Ashby MF, Evans AG, Fleck NA, Gibson LJ, Hutchinson JW, Wadley HNC. Metal foams: a design guide. Oxford: Butterworth Heinemann, 2000.